ELSEVIER

Contents lists available at ScienceDirect

# Microchemical Journal

journal homepage: www.elsevier.com/locate/microc





# Peroxidase-mimicking Pt nanodots supported on polymerized ionic liquid wrapped multi-walled carbon nanotubes for colorimetric detection of hydrogen peroxide and glucose

Li Gong <sup>a</sup>, Yang Chen <sup>c</sup>, Xiaopeng Bai <sup>a</sup>, Tianchi Xu <sup>a</sup>, Siyuan Wu <sup>b</sup>, Wenbo Song <sup>b,\*</sup>, Xun Feng <sup>a,\*</sup>

- <sup>a</sup> Department of Sanitary Inspection, School of Public Health, Shenyang Medical College, Shenyang 110034, China
- <sup>b</sup> College of Chemistry, Jilin University, Changchun 130012, China
- <sup>c</sup> Department of Pharmaceutics, School of Pharmacy, China Medical University, Shenyang, China

#### ARTICLE INFO

#### Keywords: Pt-PIL-MWCNTs Peroxidase mimetics Colorimetry H<sub>2</sub>O<sub>2</sub> Glucose

#### ABSTRACT

Pt nanoparticles have been actively researched as enzyme mimetic nanomaterials for bioanalysis, catalysis and environment treatment over the past years. However, the general issues with individual Pt nanoparticles are stabilization and reproducibility, which lead to the search of Pt based nanocomposite to enhance their activity. In this work, we developed a novel kind of surfactant-free nanocomposites (Pt-PIL-MWCNTs) containing Pt nanodots highly dispersed on polymerized ionic liquid wrapped multi-walled carbon nanotubes, and demonstrated their intrinsic peroxidase-like activity for use in colorimetric detection of hydrogen peroxide and glucose. The Pt-PIL-MWCNTs were characterized by transmission electron microscopy (TEM), scanning electron microscopy (SEM) and X-ray photoelectron spectroscopy (XPS). The as-prepared Pt-PIL-MWCNTs were used to catalyze the oxidation of a peroxidase substrate 3,3,5,5-tetramethylbenzidine (TMB) by  $\rm H_2O_2$  to the oxidized colored product. Based on the excellent catalytic activity of Pt-PIL-MWCNTs, two colorimetric sensors for detecting  $\rm H_2O_2$  and glucose, respectively, were constructed with a wide linear range of  $\rm 10$ –1000  $\mu M$  (for  $\rm H_2O_2$ ) and  $\rm 160$ –900  $\mu M$  (for glucose), as well as a relative lower limit of detection [5.5  $\mu M$  (for  $\rm H_2O_2$ ) and 50  $\mu M$  (for glucose)]. The excellent performance of the sensor exhibited that the Pt-PIL-MWCNTs composite could be used as a promising mimetic peroxidase for applications in biosensing.

### 1. Introduction

Due to the high substrate specificity and extraordinary catalytic efficiency under mild conditions, enzymes have been extensively studied and found applications in medicine, chemical industry, food processing and ariculture. However, the natural enzymes inevitably suffer from several serious drawbacks such as easy thermal denaturation, high-cost in preparation and separation, harsh catalysis reaction condition, and possible protease digestion, thus seriously restricting their widespread. To overcome these challenges, considerable efforts have been channeled toward discovering and developing new enzyme mimetics during the last few years. These enzyme mimetics are considered as the materials that bear enzyme-like activities while have excellent advantages of tunable structures, high stability, lower cost, and mature synthetic routes [1]. Among them, peroxidase-mimicking enzyme have been explored at a rapidly growing rate because of their unique potential in

disease diagnostics and therapy [2] Up to date, various mimetic peroxidases have been developed based on cyclodextrins, porphyrins, polymers, and supramolecules, which mimicked the structures and enzyme-like catalytic activities of enzymes [3,4]. Nevertheless, their unsatisfactory activity and complex synthesis have pushed scientists to identify novel and easily prepared substances with excellent catalytic activity as peroxidase mimetics.

During recent years, the growing filed of nanotechnogy has resulted in the exploitation of nanostructured materials as mimetic peroxidases, which has been defined as nanozyme [5]. In 2007, the  $Fe_3O_4$  magnetic nanoparticles were demonstrated for the first time to possess intrinsic enzyme activity similar to that found in natural peroxidases [6]. Afterwards, other nanomaterials like carbon-based nanostructures [7–9],  $Co_4N$  nanowires [10],  $V_2O_5$  nanowires [11],  $MnO_2$  nanowires [12],  $Co_3O_4$  nanoplates [13], Metal-organic frameworks (MOFs) [14,15], noble-metal nanostructures [16–18] and so on, have been reported to

E-mail addresses: wbsong@jlu.edu.cn (W. Song), fengxundfx@163.com (X. Feng).

<sup>\*</sup> Corresponding authors.

possess unique intrinsic peroxidase-like catalytic activity.

As a potential catalyst at nanoscale, noble metal platinum (Pt) element has been extensively explored for its enzyme-like catalysis activity in biological detection or superoxide free radicals elimination [19]. Until now, several Pt nanomaterials have been reported to possess peroxidase enzyme mimetic activities [20-22]. Small Pt nanostructures with high specific surface area are of particular importance for the efficient catalysis and sensitive detection. However, the small Pt nanostructure tends to aggregation, which leads to performance deterioration. So a support is often needed to keep them in a well-dispersed state [23]. Multi-walled carbon nanotubes (MWCNTs) are a class of promising one-dimensional nanomaterials. Due to their large active surface area, good conductivity and chemical stability, MWCNTs have been used as host materials for the distribution of noble nanoparticles [24]. For the MWCNTs without surface modification, there are insufficient binding sites for anchoring the precursors of Pt, which usually leads to poor dispersion and large Pt NPs. Therefore, much attention has been paid to the synthesis of PtNPs on functionalized MWCNTs.

In our previous report, we have reported a tunable thermal-initiation-free radical approach to homogeneously fabricate the surfaces of MWCNTs with thickness controllable polymeric ionic liquid (PIL). By using the imidazole group-containing ionic liquid as precursor, the surfaces of PIL-MWCNTs are terminated with abundant positive charges and increase the hydrophilicity of MWCNTs. In addition, the PIL film can serve as anchiriong points for the immobilization of Pt precursors on the surface of MWCNTs [25].

In this paper, we synthesis the ultra-fine Pt nanodots on the surface of PIL-MWCNTs using a surfactant-free method. The as-prepared Pt-PIL-MWCNTs can catalyze the oxidation of the peroxidase substrate 3, 3, 5, 5-tetramethylbenzidine (TMB) in the presence of  $\rm H_2O_2$  to exhibit a blue color change in aqueous solutions, which could be used as a colorimetric method for  $\rm H_2O_2$  and glucose determination.

### 2. Experiment

### 2.1. Reagents and apparatus

Pristine-MWCNTs (length 5–15 µm, diameter 20–40 nm) were purchased from Shenzhen Nanotech Port Co. Ltd., China. 3-ethy-1-vinylimidazolium tetrafluoroborate ([VEIM] BF4) was purchased from Lanzhou Green ILS, LICP. CAS. China. 2, 2-azobisisobutyronitrile (AIBN) was purchased from Sinopharm Chemical Reagent Co., Ltd. Chloroplatinic acid (H2PtCl6), 3,3,5,5-tetramethylbenzidine (TMB), Horseradish peroxidase (HRP), and glucose oxidases (GOx) were purchased from Sigma. Hydrogen peroxide (H2O2, 30%), glucose, fructose, lactose, and maltose were obtained from Beijing Chemical Reagent Company. All chemicals were of analytical grade and ultra-pure water was used for making the solutions. Phosphate buffer solution (0.1 M) was prepared by mixing the 0.1 M Na2HPO4 and 0.1 M NaH2PO4, and the pH was adjusted by HCl or NaOH. All solutions were freshly prepared before each experiment.

UV-vis absorption spectra were recorded on a GBC Cintra 10e UV-vis spectrophotometer (Australia). Scanning electron microscopy (SEM) images were recorded on s-4800, Hitachi. Transmission electron microscope (TEM) images were recorded on TECNAI F20. X-ray photoelectron spectroscopy (XPS) was performed on ESCALAB 250. Cyclic voltammetry (CV) and chronoamperometry were performed on a CHI 660A Electrochemical Workstation (CH Instrument, USA) with a conventional three-electrode system. Pt-PIL-MWCNTs modified glassy carbon electrode (GCE) was used as working electrode. A platinum wire was applied as the counter electrode and a saturated calomel electrode (SCE) served as reference electrode. All potential values given below were referred to SCE.

#### 2.2. Preparation of the Pt-PIL-MWCNTs

PIL-MWCNTs were synthesized according to our previously reported work [25]. Briefly, 120.0 mg pristine MWCNTs was dispersed in 20.0 mL methanol. After ultrasonication for 30 min, 180 µL of [VEIM] BF<sub>4</sub> monomer was added to the above mixed solution. 20.0 mg AIBN was then added into the mixture as the initiators in the thermal-initiationfree radical polymerization reaction. The mixture was ultrasonicated for another 30 min and then transferred to a 50.0 mL round-bottomed flask equipped with a condenser and magnetic stirrer. After the mixture was refluxed for 10 h at 353 K under vigorous stirring and N2 protection, the precipitate was filtered with a nylon 66 membrane, and washed with methanol and ethanol several times to thoroughly remove IL monomer on the MWCNT surface. The final products were dried in a vacuum oven at 333 K, resulting PIL-MWCNTs. To achieve Pt nanodots binding on PIL-MWCNTs surface, 20.0 mg of PIL-MWCNTs was mixed with 176.0  $\mu$ L H<sub>2</sub>PtCl<sub>6</sub> (193.08 mM) in 30.0 mL ethylene glycol. The pH of the solution was adjusted slightly less than 10.0 by dropping 0.1 M NaOH in ethylene glycol. After being sonicated for 30 min, the solution was placed in the microwave oven for 180 s (power: 700 W, Galanz). The product was collected and dried in an oven at 333 K, resulting Pt-PIL-MWCNTs. The synthetic route for the Pt-PIL-MWCNTs was shown in

## 2.3. Kinetic analysis and relative activity comparison

To evaluate the catalytic activity of Pt-PIL-MWCNTs, the steady-state kinetic parameters were determined by using  $\rm H_2O_2$  and TMB as substrates under the optimal conditions. The reaction was carried out at 40 °C in a 4 mL tube with Pt-PIL-MWCNTs or HRP in 2.0 mL phosphate buffer solution (0.1 M, pH4.0) in the presence of  $\rm H_2O_2$  (50.0 mM) or TMB (500.0  $\mu$ M). The assays were carried out by varying concentration of TMB at a fixed concentration of  $\rm H_2O_2$  or vice versa. The reaction kinetics measurements were carried out by recording the absorption value at 652 nm with a 1 min interval in scanning kinetics mode.

# 2.4. $H_2O_2$ and glucose detection using Pt-PIL-MWCNTs as peroxidase mimic

A typical colorimetric analysis for  $H_2O_2$  was realized as follows. Firstly,  $100.0~\mu L$  of TMB (10.0~mM),  $10.0~\mu L$  of Pt-PIL-MWCNTs ( $1.0~mg~mL^{-1}$ ) and  $50.0~\mu L$  of  $H_2O_2$  with different concentrations were added into 2.0~mL of phosphate buffer solution (0.1 M, pH 4.0). Secondly, the mixed solution was incubated in 40 °C water bath for 20 min. Finally, the resultant solution was used further for absorption spectroscopy measurement.

Glucose detection was realized as follows: 20.0  $\mu L$  of GOx (20 mg mL $^{-1}$ ) and 80.0  $\mu L$  of glucose with different concentrations in phosphate buffer solution (0.1 M, pH 7.0) were incubated at 35  $^{\circ}C$  in water bath for 20 min. Then, 30  $\mu L$  of TMB (10.0 mM), 25  $\mu L$  of Pt-PIL-MWCNTs (1.0 mg mL $^{-1}$ ), and 1.0 mL of phosphate buffer solution (0.1 M, pH 4.0) were added into the above solution, and the final mixture was further incubated at 40  $^{\circ}C$  for 20 min. Finally, the resulting solution was taken for absorption spectroscopy measurement. At the same time, the control experiments were run with fructose, maltose and lactose instead of glucose in a similar way.

To learn the specificity of Pt-PIL-MWCNTs towards glucose detection, fructose, maltose and lactose were used to replace glucose to perform the measurements under conditions in detail to above.

### 3. Results and discussion

# 3.1. Characterization of the Pt-PIL-MWCNTs

A representative low magnification SEM image of Pt-PIL-MWCNTs and corresponding C and Pt mapping were shown in Fig. 2A. The as-

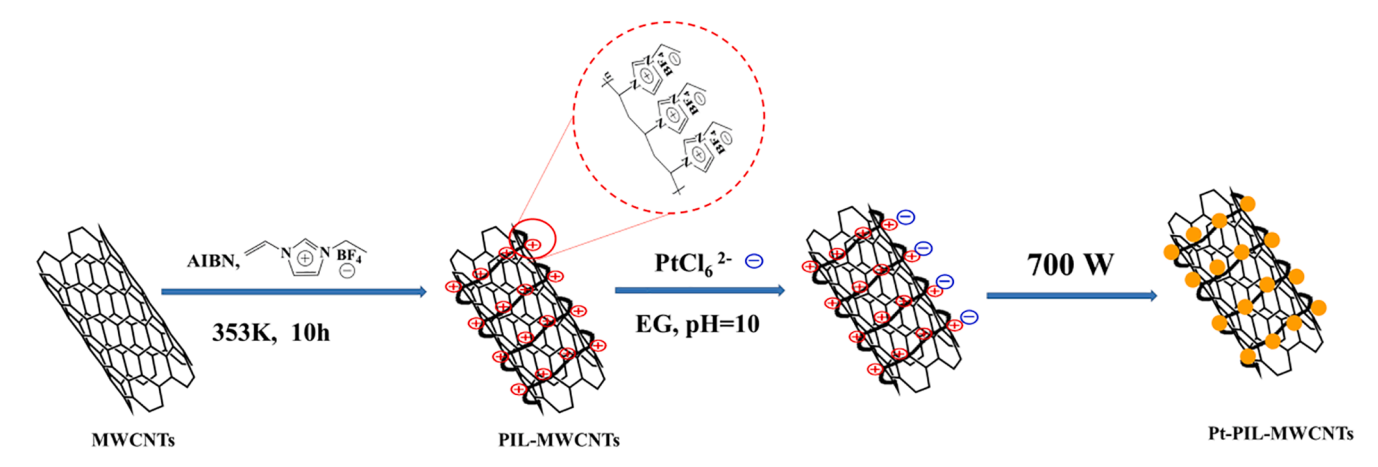


Fig. 1. Schematic diagram of the preparation processes of Pt-PIL-MWCNTs.

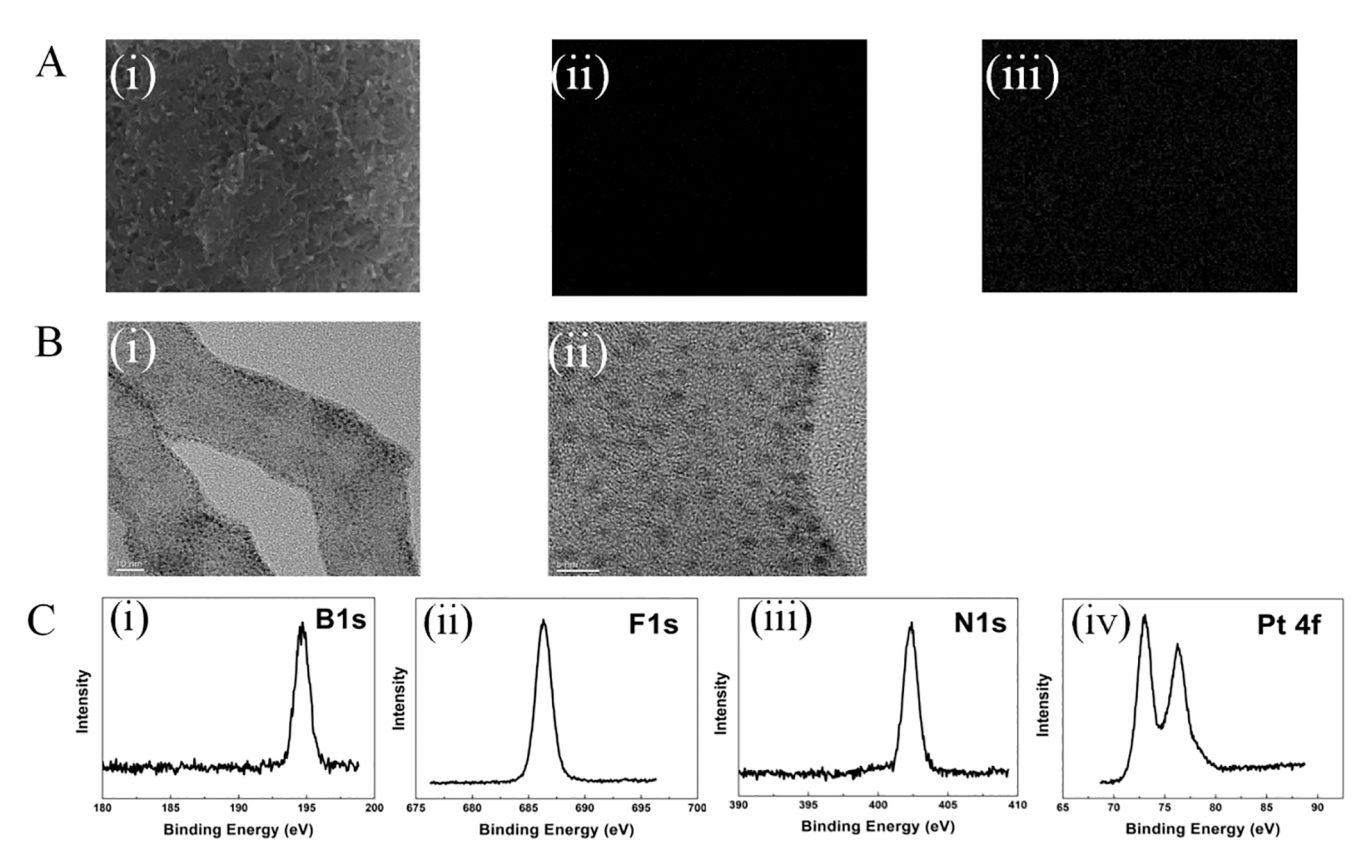


Fig. 2. (A) Lower magnified SEM image of Pt-PIL-MWCNTs (i) and the corresponding C (ii) and Pt (iii) mapping images. (B) TEM images of Pt-PIL-MWCNTs (i-ii) at different magnification. (C) XPS of B1s (i), F1s (ii), N1s (iii) and Pt 4f (iv) of Pt-PIL-MWCNTs.

prepared Pt-PIL-MWCNTs were agglomerated, and no obvious Pt nanodots were observed in this sample (Fig. 2A(i)). Energy dispersive X-ray (EDX) elemental mappings of C and Pt in this sample were displayed in Fig. 2A (ii)-(iii); homogeneous dispersions of C and Pt elements in Pt-PIL-MWCNTs were all observed. Fig. 2B (i)-(ii) showed the the high magnification TEM images of the Pt-PIL-MWCNTs. As shown, TEM images confirmed that the PIL-MWCNTs were decorated successfully with many well-dispersed PtNPs. The average size of Pt NPs was as small as around 3 nm.

The modification of MWCNTs by PIL was further confirmed by XPS as shown in Fig. 2C. The values of binding energies obtained for B1s and F1s were located at 197.4 eV (Fig. 2C (i)) and 684.4 eV (Fig. 2C (ii)), demonstrating the presence of BF $_4$  anion of PIL on the surface of MWCNTs. The N1s peak appeared at 402.5 eV (Fig. 2C (iii)), clearly

demonstrating the existence of imidazolium ring of PIL on the surface of MWCNTs. The presence of B1s, N1s and F1s confirmed the successful modification of PIL on MWCNTs surfaces via the thermal-initiation-free radial polymerization approach. The Pt 4f7/2 and 4f5/2 lines appeared at 71.5 eV and 74.8 eV (Fig. C (iv)) respectively, which supported the conclusion that Pt-PIL-MWCNTs nanohybrids had been successfully achieved.

# 3.2. The peroxidase-like catalytic activity of Pt-PIL-MWCNTs

To investigate the peroxidase-like catalytic activity of the Pt-PIL-MWCNTs, the Pt-PIL-MWCNTs-catalyzed reaction of peroxidase substrate TMB with  $\rm H_2O_2$  was tested. The activity was compared with PIL-MWCNTs and blank. As shown in the inset of Fig. 3A, the Pt-PIL-

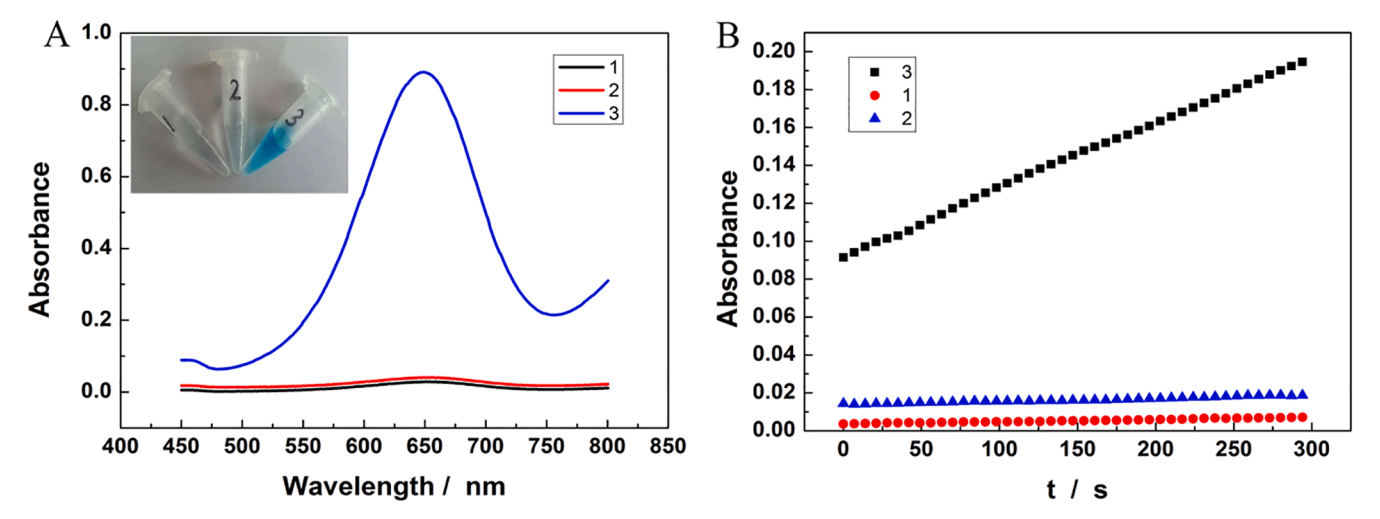


Fig. 3. (A) Typical absorption spectra of blank (1), PIL-MWCNTs (2) and Pt-PIL-MWCNTs (3). Inset of Fig. 3(A) the color of corresponding solutions. (B) The kinetic curves measuring the absence at 652 nm vs. time of blank (1), PIL-MWCNTs (2) and Pt-PIL-MWCNTs (3) in the presence of 100 mM  $H_2O_2$  and 500  $\mu$ M TMB in phosphate buffer solution (0.1 M, pH 4.0).

MWCNTs can catalyze the oxidation of TMB by H2O2 to produce the typical blue color, indicating that Pt-PIL-MWCNTs had peroxidase-like catalytic activity. The catalytic reaction could be detected by monitoring TMB absorbance change at 652 nm, resulting from the catalytic oxidation product of TMB, as shown in Fig. 3A (curve 3). However, the PIL-MWCNTs almost cannot catalyze the oxidation of TMB by H<sub>2</sub>O<sub>2</sub> as the same as the blank. Fig. 3B showed that the change of absorbance at 652 nm with reaction time. With the addition of Pt-PIL-MWCNTs, the absorbance change was greatly improved. As for PIL-MWCNTs and blank, the absorbance was unchanged. The results indicated that the mimetic peroxidase activity of Pt-PIL-MWCNTs was derived from Pt nanodots. The NPs-based peroxidase mimics in previous reports were mainly composed of metal ion compounds, in which the enzyme-like activity was debated owing to the valence variations of metal ions [26,27]. In the case of Pt nanodots, Pt has a zero valence. Therefore, the catalytic mechanism is different from aforementioned NPs. It is well known that Pt is the super catalyst for hydrogen peroxide reduction in electrocatalytic processes [28,29]. We investigated the electrocatalytic behavior of Pt-PIL-MWCNTs toward the electrochemical reduction of H<sub>2</sub>O<sub>2</sub>. As shown in Fig. S1 (Supplementary Information), upon addition of H<sub>2</sub>O<sub>2</sub>, obvious current at -0.2 V was found for Pt-PIL-MWCNTs modified GCE. The result suggested that Pt-PIL-MWCNTs possess an electrocatalytic ability to the reduction of H<sub>2</sub>O<sub>2</sub> through promoting electron transfer between the GCE and H<sub>2</sub>O<sub>2</sub>. Thus, it is very likely that the nature of peroxidase mimicking activity of our Pt-PIL-MWCNTs was attributed to their ability of facilitating electron transfer between TMB and H2O2.

The catalytic activity of Pt-PIL-MWCNTs was, like HRP, dependent on pH, temperature and H<sub>2</sub>O<sub>2</sub> concentration. We measured the peroxidase-like activity of Pt-PIL-MWCNTs while vary the pH from 2 to 10, the temperature from 20 °C to 55 °C, and the H<sub>2</sub>O<sub>2</sub> concentration from 0 to 1000.0 mM and compared the results with the activity found in HRP over the same range of parameters. The effects of these three parameters on the catalytic relative activity of TMB oxidation were shown in Fig. S2(A-C). As shown in Fig. S2(A), the maximum catalytic activity of Pt-PIL-MWCNTs and HRP were all obtained at pH 4.0. Fig.S3(A) showed that the solution appears with no color change at pH > 5.0, but obviously exhibits blue color at pH 4.0. Furthermore, it is found that the blue products are unstable as the acidity of the solution increased, because the blue products are further oxidized to yield yellow imide at pH 2.0 and pH 3.0. Accordingly, pH 4.0 was used in the following experiments. Fig.S3(B) showed the influence of catalytic reaction temperature upon the catalytic efficiency of Pt-PIL-MWCNTs. For Pt-PIL-

MWCNTs, the optimal temperature was 40 °C. If the temperature kept increasing, the catalytic activity of Pt-PIL-MWCNTs decreased, due to the decomposition of  $\rm H_2O_2$ . And the optimal temperature for HRP was 30 °C. Compared with HRP, Pt-PIL-MWCNTs was insensitivity to the reaction temperature. Fig.S2(C) showed that the Pt-PIL-MWCNTs required a  $\rm H_2O_2$  concentration two level of magnitude higher than HRP to reach the maximal level of peroxidase activity. However, further increase in the  $\rm H_2O_2$  concentration inhibited the peroxidase-like activity of the Pt-PIL-MWCNTs. The optimal  $\rm H_2O_2$  concentration for Pt-PIL-MWCNTs was 200.0 mM.

# 3.3. Kinetic analysis of Pt-PIL-MWCNTs as peroxidase mimics

To further investigate the mechanism of peroxidase-like catalytic property of Pt-PIL-MWCNTs, the apparent steady-state kinetics parameters for the mimetic peroxidase reaction were determined. The corresponding kinetic data were obtained by varying one substrate concentrations while fixing the other substrate concentration constant. As shown in Fig. S4(A-B), within the suitable range of either substrate concentration, typical Michaelis-Menten curves were obtained for Pt-PIL-MWCNTs by dividing the absorbance by the molar absorption coefficient (39,000  $\rm M^{-1}cm^{-1})$  of TMB-derived oxidation product. The related data were fitted to the Michaelis-Menten model. The Michaelis-Menten constant ( $\rm K_m$ ), which is an indicator of enzyme affinity for its substrate, was obtained by using Lineweaver-Burk plot:

$$\frac{1}{v} = \left(\frac{K_m}{V_{max}}\right) \left(\frac{1}{[S]}\right) + \left(\frac{1}{V_{max}}\right)$$

where  $\nu$  is the initial velocity, [S] is the concentration of the substrate, and  $V_{max}$  is the maximal reaction velocity and Km is the Michaelis constant. The corresponding kinetic parameters were compiled in Table S1. As a control, the peroxidase reaction performances of HRP were also measured. From Table S1, one can see that with  $H_2O_2$  as the substrate, the apparent Km value of Pt-PIL-MWCNTs is significantly higher than that for HRP. This results is consistent with the fact that a higher  $H_2O_2$  concentration was required to achieve maximal activity for Pt-PIL-MWCNTs. While with TMB as the substate, the Km value of Pt-PIL-MWCNTs is similar to that of HRP, suggesting a comparable affinity to TMB for Pt-PIL-MWCNTs and HRP.

# 3.4. Determination of $H_2O_2$ and glucose using the peroxidase like catalytic reaction of Pt-PIL-MWCNTs

Based on the intrinsic peroxidase-like activity of Pt-PIL-MWCNTs, an efficient and fast colorimetric method for the detection of  $\rm H_2O_2$  was created under optimum assay conditions. As shown in Fig. 4A, the absorbance of the oxidized TMB at 652 nm increased gradually with the increase of  $\rm H_2O_2$  concentration. From Fig. S5A, the absorbance at 652 nm showed a good linear relationship with the concentration of  $\rm H_2O_2$  ranging from 10 to 1000  $\mu M$  and a detection limit of 5.5  $\mu M$  (S/N = 3).

Since glucose can be oxidized to produce gluconic and  $H_2O_2$  after the reaction with GOx and  $O_2$ , so a highly selective and sensitive glucose colorimetric method can be established by using above TMB system. As presented in Fig. 4B, the absorbance at 652 nm increased with the increased glucose concentration. The typical linear response between absorbance and concentration of glucose in a range from 160 to 900  $\mu M$  (Fig. S5B) was obtained. The detection limit was calculated to be 50  $\mu M$  (S/N = 3). Moreover, we compared peroxidase mimic performance of Pt-PIL-MWCNTs with other nanomaterials using colorimetric detection of  $H_2O_2$  and glucose, which was shown in Table S2. It was found that the developed method in this study was comparable or more sensitive than some previously proposed systems.

The selectivity of the proposed method was also studied. The absorbance responses of three glucose analogs, lactose, fructose, and

maltose, were monitored and compared with that of glucose. Fig. 4C showed that the addition of 0.9 mM glucose results in a remarkable increase in absorbance. Moreover, the blue color change induced by glucose can be easily distinguished by the naked eyes. In contrast, negligible absorbance change was observed even after adding 9 mM fructose, lactose, or maltose. This indicated that the present biosensing system had high selectivity for glucose.

To explore the biocompatibility and the feasibility of Pt-PIL-MWCNTs sensing system in practical applications, detection of glucose in human blood serum samples were further performed. In our experiments, the concentrations of glucose for two diluted human blood serum samples were estimated to be  $4.55\pm0.12~\text{mM}~(n=3)$  and  $8.69\pm0.20~\text{mM}~(n=3)$ , which are in good agreement with the values (4.60 and 8.60 mM) measured by the School Hospital of Jilin University. The relative standard deviation of three repeated measurements was within the range of 1.79–3.13%. All these results demonstrated that the colorimetric method based on Pt-PIL-MWCNTs is precision, biocompatible and reliable on practical determination of glucose for future practical in both healthy persons and diabetic patients.

#### 4. Conclusion

In summary, Pt-PIL-MWCNTs nanozyme was prepared and investigated as peroxidase mimetics. The catalytic oxidation of substrate TMB

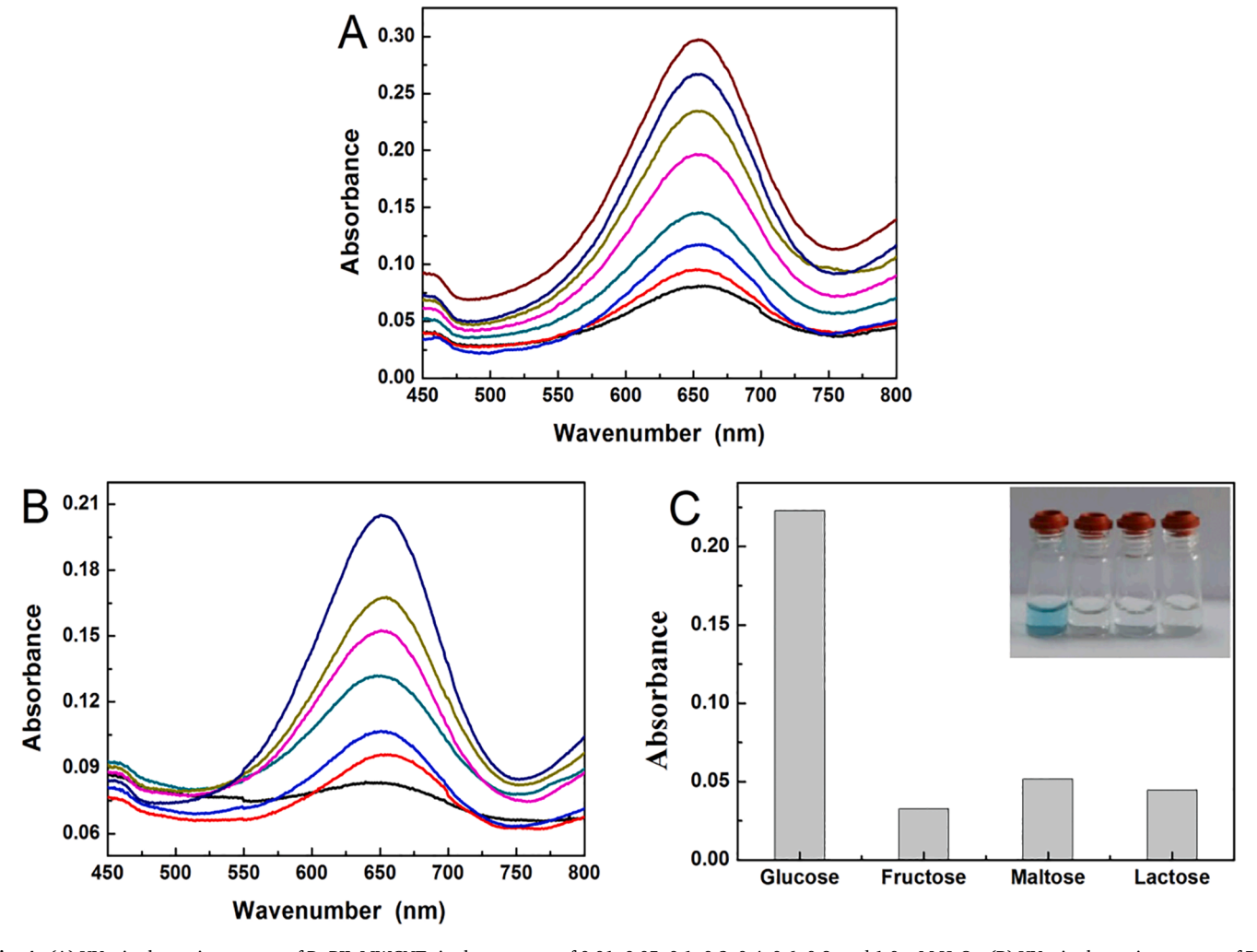


Fig. 4. (A) UV–vis absorption spectra of Pt-PIL-MWCNTs in the presence of 0.01, 0.05, 0.1, 0.2, 0.4, 0.6, 0.8, and 1.0 mM  $H_2O_2$ . (B) UV–vis absorption spectra of Pt-PIL-MWCNTs in the presence of 0.16, 0.2, 0.3, 0.4, 0.6, 0.7, and 0.9 mM glucose. (C) The absorbance at 652 nm of the system with lactose, fructose, maltose (the concentration of each interferent was 9 mM), while the concentration of glucose was 0.9 mM. Inset of Fig. 4(C): Color change with the corresponding substances (from left to right: glucose, fructose, maltose and lactose).

with  $H_2O_2$  using the Pt-PIL-MWCNTs was realized. The Pt-PIL-MWCNTs nanozyme provided a colorimetric assay which showed good response towards  $H_2O_2$  detection. Given the promising results, a sensitive and selective analytical platform for glucose detection was fabricated based on GOx and the as-prepared Pt-PIL-MWCNTs nanozyme. The glucose sensor system constructed in the study was shown to be anti-intereference from other spices. More importantly, the Pt-PIL-MWCNTs nanozyme could rival natural enzymes due to its easy preparation, robustness, and stability. Above all, our work provides a new nanozyme that may display important applications in environment chemistry, biotechnology and medicine.

#### CRediT authorship contribution statement

Li Gong: Investigation. Yang Chen: Investigation, Writing - review & editing. Xiaopeng Bai: Investigation, Funding acquisition. Tianchi Xu: Investigation. Siyuan Wu: Investigation. Wenbo Song: Supervision, Conceptualization. Xun Feng: Supervision, Project administration, Writing - review & editing, Funding acquisition.:

#### **Declaration of Competing Interest**

The authors declare that they have no known competing financial interests or personal relationships that could have appeared to influence the work reported in this paper.

### Acknowledgments

This work was supported by the Natural Science Foundation of Liaoning Province (NO. 2020-MS-310) and Undergraduate Project of Shenyang Medical College (NO. 20198014).

# Appendix A. Supplementary data

Supplementary data to this article can be found online at https://doi.org/10.1016/j.microc.2020.105872.

# References

- [1] E. Kuah, S. Toh, J. Yee, Q. Ma, Z. Gao, Enzyme mimics: advances and applications, Chem. Eur. J. 22 (25) (2016) 8404–8430, https://doi.org/10.1002/ chem 201504394
- [2] Z. Li, X. Yang, Y. Yang, Y. Tan, Y. He, M. Liu, X. Liu, Q. Yuan, Peroxidase-mimicking nanozyme with enhanced activity and high stability based on metal-support interactions, Chem. Eur. J. 24 (2) (2018) 409–415, https://doi.org/10.1002/chem.201703833.
- [3] J. Wei, E. Wang, Nanomaterials with enzyme-like characteristics (nanozymes): next-generation artificial enzymes, Chem. Soc. Rev. 42 (2013) 6060–6093.
- [4] Q. Wang, H. Wei, Z. Zhang, E. Wang, S. Dong, Nanozyme: an emerging alternative to natural enzyme for biosensing and immunoassay, Trends Anal. Chem. 105 (2018) 218–224.
- [5] S. Jin, C. Wu, Z. Ye, Y. Ying, Designed inorganic nanomaterials for intrinsic peroxidase mimics: a review, Sensors Actuators B: Chemical 283 (2019) 18–34, https://doi.org/10.1016/j.snb.2018.10.040.
- [6] L. Gao, J. Zhuang, L. Nie, J. Zhang, Y.u. Zhang, N. Gu, T. Wang, J. Feng, D. Yang, S. Perrett, X. Yan, Intrinsic peroxidase-like activity of ferromagnetic nanoparticles, Nat. Nanotech 2 (9) (2007) 577–583, https://doi.org/10.1038/nnano.2007.260.
- [7] Y. Zhu, J. Wu, L. Han, X. Wang, W. Li, H. Guo, H. Wei, Nanozyme sensor arrays based on heteroatom-doped graphene for detecting pesticides, Anal. Chem. 92 (11) (2020) 7444–7452, https://doi.org/10.1021/acs.analchem.9b05110.s001.
- [8] M.S. Kim, S. Cho, S.H. Joo, J. Lee, S.K. Kwak, M.I. Kim, J. Lee, N-and B-codoped graphene: a strong candidate to replace natural peroxidase in sensitive and selective bioassays, ACS Nano 13 (2019) 4312–4321.

- [9] Y. Hu, X.J. Gao, Y. Zhu, F. Muhammad, S. Tan, W. Cao, S. Lin, Z. Jin, X. Gao, H. Wei, Nitrogen-doped carbon nanomaterials as highly active and specific peroxidase mimics, Chem. Mater. 30 (18) (2018) 6431–6439, https://doi.org/ 10.1021/acs.chemmater.8b02726.s001.
- [10] Y. Li, T. Li, W. Chen, Y. Song, Co<sub>4</sub>N nanowires: noble-metal-free peroxidase mimetic with excellent salt-and temperature-resistant abilities, ACS Appl. Mater. Interfaces. 9 (2017) 29881–29888.
- [11] R. André, F. Natálio, M. Humanes, J. Leppin, K. Heinze, R. Wever, H.-C. Schröder, W.E.G. Müller, W. Tremel, V<sub>2</sub>O<sub>5</sub> nanowires with an intrinsic peroxidase-like activity, Adv. Funct. Mater. 21 (3) (2011) 501–509, https://doi.org/10.1002/adfm.201001302.
- [12] L. Han, P. Liu, H. Zhang, F. Li, A. Liu, Phage capsid protein-directed MnO 2 nanosheets with peroxidase-like activity for spectrometric biosensing and evaluation of antioxidant behaviour, Chem. Commun. 53 (37) (2017) 5216–5219, https://doi.org/10.1039/C7CC02049J.
- [13] Q. Wang, J. Chen, H. Zhang, W. Wu, Z. Zhang, S. Dong, Porous Co<sub>3</sub>O<sub>4</sub> nanoplates with pH-switchable peroxidase- and catalase-like activity, Nanoscale 10 (2018) 19140.
- [14] M.-Y. Shi, M. Xu, Z.-Y. Gu, Copper-based two-dimensional metal-organic framework nanosheets as horseradish peroxidase mimics for glucose fluorescence sensing, Analytica Chimica Acta 1079 (2019) 164–170, https://doi.org/10.1016/j. aca.2019.06.042.
- [15] I. Nath, J. Chakraborty, F. Verpoort, Metal organic frameworks mimicking natural enzymes: a structural and functional analogy, Chem. Soc. Rev. 45 (2016) 4127–4170
- [16] Q. Wang, L. Zhang, C. Shang, Z. Zhang, S. Dong, Triple-enzyme mimetic activity of nickel-palladium hollow nanoparticles and their application in colorimetric biosensing of glucose, Chem. Commun. 52 (2016) 5410.
- [17] Y. Jv, B. Li, R. Cao, Positively-charged gold nanoparticles as peroxidiase mimic and their application in hydrogen peroxide and glucose detection, Chem. Commun. 46 (42) (2010) 8017, https://doi.org/10.1039/c0cc02698k.
- [18] X.-X. Wang, Q.i. Wu, Z. Shan, Q.-M. Huang, BSA-stabilized Au clusters as peroxidase mimetics for use in xanthine detection, Biosensors Bioelectronics 26 (8) (2011) 3614–3619, https://doi.org/10.1016/j.bios.2011.02.014.
- [19] M. Ma, Y. Zhang, N. Gu, Peroxidase-like catalytic activity of cubic Pt nanocrystals, Colloids Surf A 373 (2011) 6–10.
- [20] W. Shi, H. Fan, S. Ai, L. Zhu, Honeycomb-like nitrogen-doped porous carbon supporting Pt nanoparticles as enzyme mimic for colorimetric detection of cholesterol, Sensors and Actuators B: Chemical 221 (2015) 1515–1522, https:// doi.org/10.1016/j.snb.2015.06.157.
- [21] L. Jin, Z. Meng, Y. Zhang, S. Cai, Z. Zhang, C. Li, L.i. Shang, Y. Shen, Ultrasmall Pt nanoclusters as robust peroxidase mimics for colorimetric detection of glucose in human serum, ACS Appl. Mater. Interfaces 9 (11) (2017) 10027–10033, https://doi.org/10.1021/acsami.7b01616.s001.
- [22] C. Peng, Y. Zhang, L. Wang, Z. Jin, G. Shao, Colorimetric assay for the simultaneous detection of Hg<sup>2+</sup> and Ag<sup>+</sup> based on inhibiting the peroxidase-like activity of coreshell Au@Pt nanoparticles, Anal. Methods 9 (2017) 4363.
- [23] X. Liu, H. Feng, R. Zhao, A novel approach to construct a horseradish peroxidase/ hydrophilic ionic liquids/Au nanoparticles dotted titanate nanotubes biosensor for amperometric sensing of hydrogen peroxide, Biosens. Bioelectron. 31 (2012) 101–104.
- [24] B. Wu, Y. Kuang, X. Zhang, J. Chen, Noble metal nanoparticles/carbon nanotubes nanohybrids: synthesis and applications, Nano Today 6 (1) (2011) 75–90, https://doi.org/10.1016/j.nantod.2010.12.008.
- [25] X. Feng, W. Gao, S. Zhou, H. Shi, H. Huang, W. Song, Discrimination and simultaneous determination of hydroquinone and catechol by tunable polymerization of imidazolium-based ionic liquid on multi-walled carbon nanotube surfaces, Anal. Chimica Acta 805 (2013) 36–44, https://doi.org/ 10.1016/j.aca.2013.10.044.
- [26] T. Pirmohamed, J.M. Dowding, S. Singh, B. Wasserman, E. Heckert, A.S. Karakoti, J.E.S. King, S. Seal, W.T. Self, Nanoceria exhibit redox state-dependent catalase mimetic activity, Chem. Commun. 46 (16) (2010) 2736, https://doi.org/10.1039/ b922024k.
- [27] E.G. Heckert, A.S. Karakoti, S. Seal, W.T. Self, The role of cerium redox state in the SOD mimetic activity of nanoceria, Biomaterials 29 (18) (2008) 2705–2709, https://doi.org/10.1016/j.biomaterials.2008.03.014.
- [28] Y. Zhong, M. Liu, Y. Chen, Y. Yang, L. Wu, F. Bai, Y. Lei, F. Gao, A. Liu, A high-performance amperometric sensor based on a monodisperse Pt-Au bimetallic nanoporous electrode for determination of hydrogen peroxide released from living cells, Microchim. Acta 187 (2020) 499.
- [29] Y. Zhang, Q. Cao, F. Zhu, H. Xu, Y. Zhang, W. Xu, X. Liao, An amperometric hydrogen peroxide sensor based on reduced graphene oxide/carbon nanotubes/Pt NPs modified glassy carbon electrode, Int. J. Electrochem. Sci. 15 (2020) 8771–8785.